UTILIZING THE IMMERSED BOUNDARY METHOD TO ADDRESS RADIATIVE HEAT TRANSFER CHALLENGES

Saritha Sambu[1] (Research Scholar)
Dr. Manoj Singh[2] (Research Supervisor)
Department of Mathematics
[1,2] Sikkim Professional University, Gangtok, (Sikkim)

Abstract
This study represents the pioneering application of the "immersed boundary method (IBM)" to the simulation of radiative heat transport in "complex geometries. Pseudo time stepping" was employed alongside the "finite volume technique (FVM)" to solve the "radiative transfer equation (RTE)". Sharp forced interfaces were also used by IBM. This method was tested in both its two types of heat transmission modes: mixed radiant-conductive and pure reactive. The impact of the absorbent coefficient and various conduction-radiation characteristics upon the isomers and heat transfer concentration in a closed system with internal complex entities was then investigated. Results proved the method's value in dealing with radiative heat transport problems in extremely non-trivial geometries. Given that the calculations for radiative transport and energies may be solved on either the Eulerian or the LaGrange grid, coupled heat transfer problems do not necessitate the use of a third grid.
Keywords: *"Immersed boundary method; Radiative heat transfer; FVM; Sharp interface"*

Introduction

Energy transfer in "power plants, combustion chambers, high-temperature heat exchangers, rockets, etc". all rely on radiant heat transfer to some extent **(Didier, Hubert, & Patrice, 2019).** Radiative heat transport is typically modeled using the radiative transfer equation (RTE). The Zonal approach, the "Discrete Ordinate method (SN approximation), Mont Carlo, the Spherical Harmonics method (PN approximation)", and the Meshless method have all been offered as solutions to RTE **(Dhurandhar,et al 2021).** The SN approximation is the most often used of these techniques. The CFD (computational fluid dynamics) program is where you'll most often find it in use. "The finite volume method (FVM) and the discrete ordinate method (DOM)" are two of the most used approaches to SN approximation. "Discrete transfer method (DTM)", "modified discrete ordinate method (MDOM)", Flux method, and "YIX method" are all examples of techniques that rely on the SN approximation. RTE can be difficult to solve because of the difficulty of applying the boundary condition in the complicated geometries. Researchers have offered a variety of solutions to this issue, all of which are based on the "SN approximation". The blocked-off method is the quickest and most simplistic, but also the least precise. This technique uses straight lines to represent stair-step geometry in complicated boundary models **(Moghadassian, et al., 2019).**
The blocked-off technique was then proposed to be improved upon by using the embedded boundary method **(Abaszadeh, et al., 2019),** which models complicated boundaries in a "Cartesian grid". Additionally, "SN approximation" has been created for "Non-Cartesian grids" When complicated constraints are matched by the grid of cells, such as the "body-fitted structure, the multi-block grids, etc".
The immersed boundary approach (IBM) is powerful for CFD solutions. A lot of attention has been paid to it recently. This technique has helped solve fluid, aerodynamics, heat and mass transport, multiphase and particle flows, and "fluid-solid interaction (FSI)" in complex geometries. This technology's grid generation ease and memory and processor power utilization are advantages. IBM links Eulerian and Lagrangian variables with an interaction equation. Eulerian and Lagrangian variables are created on Cartesian and curved grids, respectively. We can now model heart valve blood flow thanks to Peskin's work. IBM enforces the boundary requirement by distributing a Lagrangian-point internal force on Eulerian points. IBM techniques Robin, Dirichlet, and Neumann are related, but their internal force and semi-explicit boundary condition computation methods differ. IBM's

flexibility in supporting discrete governing equations has led many researchers to use IBM with FVM, FEM, FDM, LBM, etc. We used it to simulate radiative heat transport in nontrivial geometries because of its numerous uses. A crisp direct-forced interface achieves this. For the first time, researchers suggest leveraging IBM to solve radiative heat transport problems.

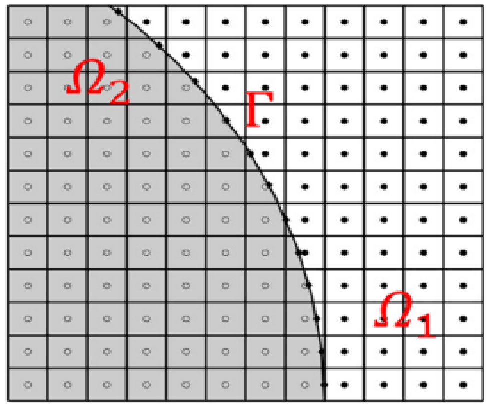

Fig. 1.1. "Schematic of the immersed boundary method" (Hu,et al 2019)

Immersed boundary method

Figure 1.1 presents IBM on a Cartesian coordinate system. "The Eulerian and Lagrangian grids" are used in conjunction with an interface method to form the "Immersed Boundary Method (IBM)". IBM's approach for enforcing curved boundary conditions is non-local since it does not involve adjusting control volumes in the boundary area but rather by adding source terms to the formulas that govern. When using the direct force strategy or the constructive forcing methods, the source term is calculated. The grid size and computing needs will dictate whether you utilize diffuse or crisp interfaces.

This study used a direct forcing approach with a crisp interface to lessen the burden on computers and prevent unnecessary rounding off. The procedure of enforcing boundary conditions on complex borders in radiative issues begins with the identification of forcing nodes (f-nodes) in the inactive part of the Eulerian grid that have at least one adjacent point in the active region. After determining the source terms for the radiation intensity at the f-nodes, the wall boundary conditions (I_W) are applied at the w-nodes of the Lagrangian grid.).

Since Eq. (1.1) now includes the source term Q_{IB}^m, for enforcing IBM, Eq. (1.3) is modified as follows:

For example:

$$\frac{1}{k_t}\frac{\partial I}{\partial t} + s_x\frac{\partial I}{\partial x} + s_y\frac{\partial I}{\partial y} = -\beta I + \sigma_a I_b + \frac{\sigma_s}{4\pi}\int_{4\pi} I(r,s')\Phi(s',s)d\Omega' .. (1.1)$$

Because of the need to keep the equation to a single dimension, the number 1 is arbitrarily chosen for the parameter k_t which has a unit of meters per second.

$$I_p^m(t) = \frac{I_{x,i}^m(t)|D_x^m|A_x + I_{y,i}^m(t)\left|D_y^m\right|A_y + \left[Q_B^m + \beta S^m(t) + I_p^m(t-\Delta t)/k_t\Delta t\right]V\Delta\Omega^m}{|D_x^m|A_x + \left|D_y^m\right|A_y + (1 + 1/k_t\Delta t)\Delta\Omega^m V} .. (1.2)$$

where

$$Q_{1B}^m = \frac{(I^m - I^m)}{k_t\Delta t} + \left[\left[I_{x,i}^m(t) - I_p^m(t)\right]|D_x^m|A_y + \left[I_{y,i}^m(t) - I_p^m(t)\right]\left|D_y^m\right|A_y\right] / .. (1.3)$$
$$\Delta\Omega^m V + \beta(I^m(t) - S^m(t))$$

The required radiation intensity $\ddot{I}^m$ is calculated using the interpolation approach in Eq. (1.3). We employed an interpolation technique in our study. In this approach, the f-nodes are split in half. Both adjacent spots in the first set are inside the dynamic range. For these data points, we employ the bilinear interpolation technique. In contrast, the linear interpolation technique is employed for the second set since only one nearby point lies within the active subdomain. The steps involved in calculating $\ddot{I}^m$ via the interpolation approach are shown in Eqs. (1.4-1.5).

$$\tilde{I}^m = \frac{1}{\delta_x \delta_y}\left(I_w^m - \left[\delta_x(1-\delta_y)I_1^m + (1-\delta_x)(1-\delta_y)I_2^m + \delta_y(1-\delta_x)I_3^m\right]\right) .. (1.4)$$

$$I^m = \begin{cases} (1-2\delta)I_w^m + 2\delta I_1^m & \delta < 0.5 \\ 2\delta I_w^m - 2\delta I_1^m - (1-2\delta)I_2^m & \delta > 0.5 \end{cases} .. (1.5)$$

"For the f-nodes at the sharp interface", interpolation happens in both groups (as described above), as depicted by the stencil in Fig. 2. For the first set, w-node is the point where the immersed boundary meets the line that passes through f-node at right angles to it. Note that $\delta x = (x_3 - x_w)/(x_3 - x_f)$ and $\delta y = (y_3 - y_w)/(y_3 - y_f)$. "For the second set, w-node is the point where the immersed boundary" meets the line that passes through f-node and its neighbor. The value of is found by dividing $(x_1 - x_w)/(x_1 - x_f)$.

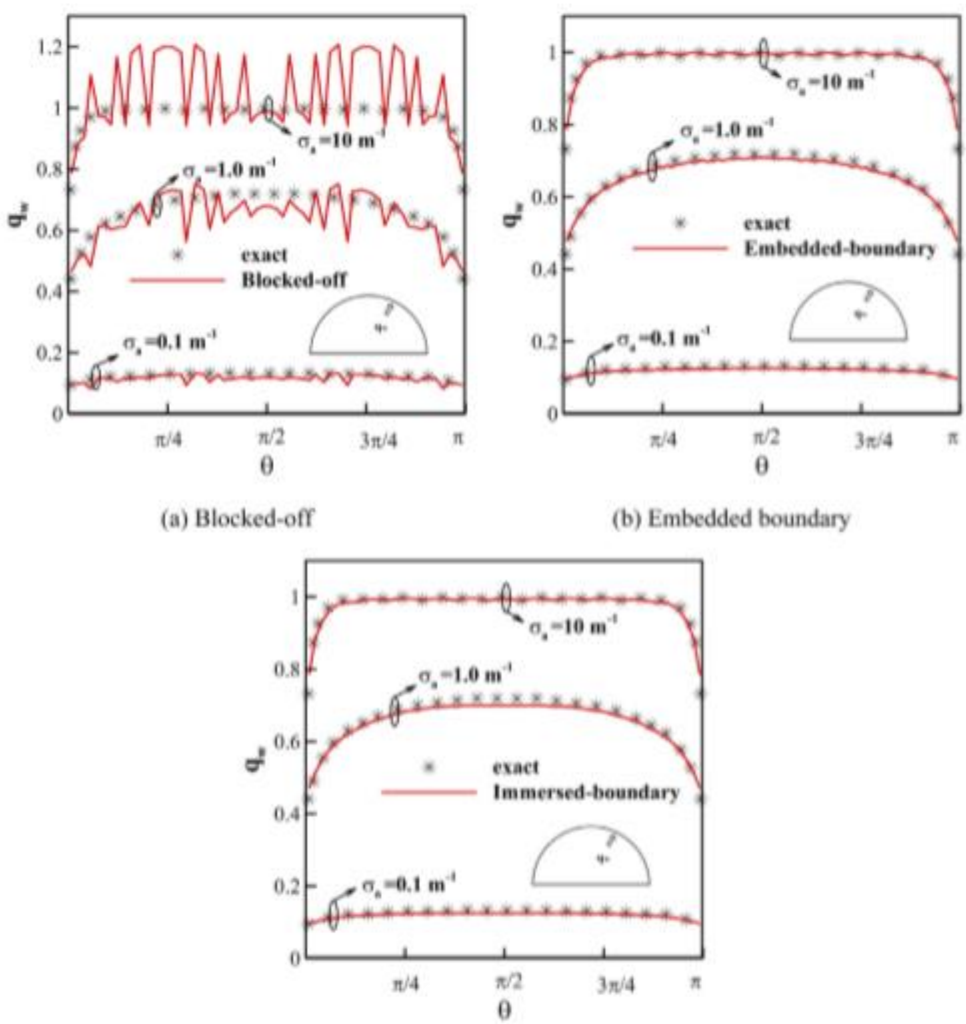

(a) Blocked-off

(b) Embedded boundary

IJFANS INTERNATIONAL JOURNAL OF FOOD AND NUTRITIONAL SCIENCES
ISSN PRINT 2319 1775 Online 2320 7876
 UGC CARE Listed (Group -I) Journal Volume 11, Iss 12, 2022

Fig. 1.2. Comparing the top wall's indeterminate radiative temperature uniformity for different numbers of σ_a. (Abaszadeh, et al., 2019)

Result

The effectiveness of this technique is tested on two standard issues involving pure radiative heat transfer. The first issue is a semicircular chamber containing a circular cylinder. The exterior walls are entirely black and kept at an average temperature of $T_w = 0(\mathrm{~K})$, while the medium is kept at a constant temperature of $T_g = 1000(\mathrm{~K})$. and does not scatter light. $N_x \times N_y \times N_\theta \times N_\emptyset = 80 \times 40 \times 4 \times 24$. is the number of spatial and angular subdivisions. The contrast between the accurate solution and the dispersion during the bottom wall's indeterminate radiated heat flow is seen in Fig. 1.3b.

In this research, the radiative heat transfer problems were simulated using IBM and the pseudo time stepping approach was employed to solve RTE. For this reason, we compare the times required by the time-stepping pseudo-solver employing steadystate solver to complete the same benchmark task.

An enclosure of side $L = 1(\mathrm{~m})$ is considered, with the top wall being hot at a constant temperature $T_h = 1000(K)$, and the remaining walls being cool at a constant temperature $T_C = O(K)$.

"Radiative equilibrium with pure scattering" ($\sigma_s = 10\ \mathrm{m}^{-1}$). is also assumed for the medium. A uniform 100x100 "grid, with angular divisions" of $N_h \times N_0 = 4 \times 24$, is used to study the square medium.

Table 1 shows that when compared to the steady-state solver, The time response and the total number of rounds over each of the 4-time phases only slightly differ from one another. Therefore, it follows that the false time shifting approach doesn't significantly slow down the final answer. As a linear solver, Eq. (1.2) may be used to determine the radiant intensity in a material that is actively absorbing or reflecting light.

We will examine the effects on heat transfer in the "pure radiative and mixed radiative-conductive" regimes when the geometry of the cylinders inside the square enclosure is varied. The three shapes that have been looked at are a circle, an ellipse, and a clover with three leaves. All of these people fit inside a circle whose radius is r=0.2(" " m). A ratio of 2 between ellipse sizes was also assumed. All three cases studied are shown in Fig. 10.

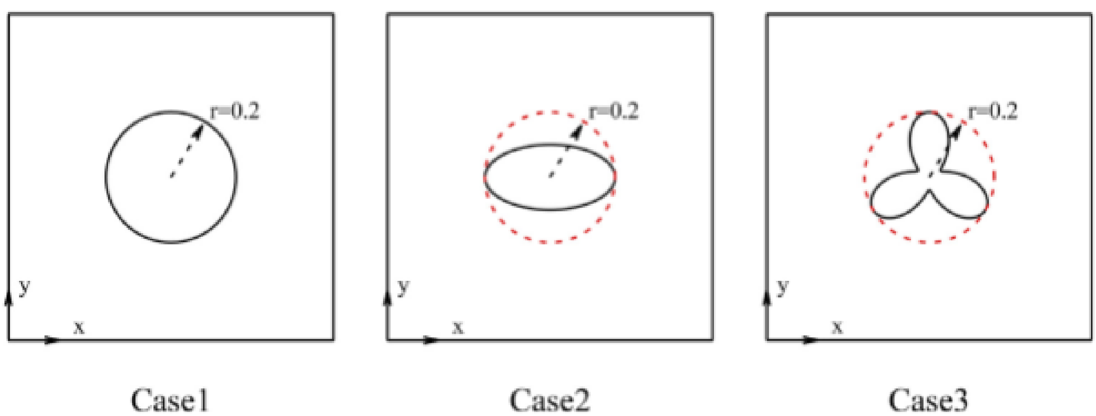

Fig. 1.3. "Schematic of the square enclosure with different internal cylinder's shapes".

Conclusion

This study represents the pioneering "application of the immersed boundary method (IBM)" to problems in radiative heat transport. We find that include a spurious temporal element in the "radiative transfer equation (RTE)" solution does not significantly increase or decrease the time needed to complete the calculation. Our immersed boundary technique (IBM) was shown to outperform the "embedded boundary and blocked-off approaches", and it provided a more uniform distribution of radiative heat flux along the curved wall. Additionally, the problem of coupled heat transfer was tackled by employing the "immersed boundary method (IBM)". The results indicate that this approach is promising for dealing with the aforementioned problems. One important part of this method for handling coupled heat transfer issues is the use of a single grid for both radiative and temperature computations.

Reference

Didier, Y. E. H., Hubert, B. B. G., & Patrice, E. A. (2019). Solution of the one-speed neutron transport equation in anisotropic scattering medium with a Pomraning-Eddington approximation approach. *Journal of Physics Communications*, *3*(5), 055016.

Dhurandhar, S. N., Bansal, A., Boppudi, S. P., & Murty Kadiyala, M. D. (2022). Application and comparative analysis of radiative heat transfer models for coal-fired furnace. *Numerical Heat Transfer, Part A: Applications*, *82*(4), 137-168.

Moghadassian, B., Jafari, M., Hafezisefat, P., Mirhosseini, M., & Rezania, A. (2019). Numerical investigation of radiative heat transfer inside a 2-D irregular geometry containing nano-and micro-size particles. *Energy Procedia*, *158*, 5685-5691.

Abaszadeh, M., Safavinejad, A., Delouei, A. A., & Amiri, H. (2022). Analysis of radiative heat transfer in two-dimensional irregular geometries by developed immersed boundary–lattice Boltzmann method. *Journal of Quantitative Spectroscopy and Radiative Transfer*, *280*, 108086.

Hu, Y., Li, D., Niu, X., & Shu, S. (2019). An immersed boundary-lattice Boltzmann method for electro-thermo-convection in complex geometries. *International Journal of Thermal Sciences*, *140*, 280-297.